Geoderma 440 (2023) 116709

Contents lists available at ScienceDirect

Geoderma

journal homepage: www.elsevier.com/locate/geoderma

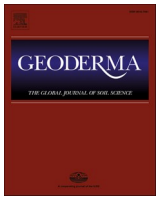

Contributions of fine mineral particles and active Al/Fe to stabilization of plant material in neutral-to-alkaline soils of Indo-Gangetic Plain

Ruohan Zhong [a], Han Lyu [a,b,*], Monika Kumari [b], Ajay Kumar Mishra [b], M.L. Jat [c,d], Randy A. Dahlgren [e], Shinya Funakawa [a,b], Tetsuhiro Watanabe [a,*]

[a] Graduate School of Agriculture, Kyoto University, Kyoto 606-8502, Japan
[b] Graduate School of Global Environmental Sciences, Kyoto University, Kyoto 606-8501, Japan
[c] International Crops Research Institute for the Semi-Arid Tropics, Patancheru 502324, Telangana, India
[d] International Maize and Wheat Improvement Center, India Office, National Agricultural Science Centre Complex, New Delhi 110012, India
[e] Department of Land, Air and Water Resources, University of California Davis, Davis 95616, CA, USA

ARTICLE INFO

Handling Editor: Pauline Chivenge

Keywords:
Soil organic matter
Fractionation
^{13}C tracing
Pyrolysis-GC/MS
Clay and silt
Topsoil and subsoil

ABSTRACT

Factors controlling organic carbon stabilization are elusive in neutral-to-alkaline soils, thereby hindering the assessment of carbon sequestration potential across vast agricultural regions like the Indo-Gangetic Plain (IGP). This study investigated controls over mineralization and stabilization of added organic matter in tropical neutral-to-alkaline soils with low organic carbon (SOC). Using topsoil and subsoil samples from 12 sites of upper-to-lower IGP, we conducted a one-year incubation with and without adding ^{13}C-labeled maize material. We tracked CO_2 release and residual C remaining in soil organic matter fractions (free, occluded particulate (oPOM), and mineral-associated organic matter (MAOM)) and analyzed organic matter molecular compositions in incubated soils using pyrolysis-GC/MS. Our results revealed that 48 ± 7 % of added maize C was mineralized, mostly within the first 70 days. Higher active Al/Fe, notably Al, retarded primary maize mineralization by facilitating aggregation. High SOC content and SOC saturation degree resulted in more maize mineralization. The disappearance of maize-unique compounds (e.g., neophytadiene) revealed substantial degradation of added maize. Regarding SOC composition, maize addition increased the relative abundance of fatty acids and decreased that of N-containing compounds. Most residual maize-derived C was found in stabilized fractions, MAOM (77 ± 15 % of residual maize C) and oPOM (8 ± 4 %). Clay fraction contributed to most maize-derived C stabilization as MAOM (path coefficient (β) = 0.81**). Moreover, the significant correlation ($P < 0.001$) between maize-derived oPOM C and active Al/Fe or clay + silt suggested that active Al/Fe contributed to the stabilization of maize-derived C as oPOM (β = 0.62***) probably by bonding clay and silt particles to form stable aggregates since active Al/Fe content was low (<14 cmol kg^{-1}). Our study highlighted the importance of active Al/Fe in stabilizing SOC, by promoting aggregation and retarding degradation of residue-derived C in neutral-to-alkaline soils.

1. Introduction

Soil organic carbon (SOC) is the largest carbon pool in terrestrial ecosystems (Jobbagy and Jackson, 2000) and plays a key role in controlling carbon cycling, soil health, and agricultural production. Severe depletion of the SOC pool degrades several ecosystem services, such as climate regulation, food/fiber/forage production, and water quality (Lal, 2018). SOC depletion may be further exacerbated by global warming, thereby creating a positive feedback loop of diminishing SOC. Moreover, land-use change from native to agricultural ecosystems can lead to a pronounced decrease in the SOC pool by up to 60 % in temperate soils and 75 % or more in tropical soils (Lal, 2010). Many tropical soils are deficient in inorganic nutrients, hence maintaining soil fertility relies critically on the recycling of nutrients through the soil organic matter (SOM) (Lu, 2021; Tiessen et al., 1994). Consequently, soil organic carbon conservation and restoration are especially crucial to sustainable land use in the tropics.

The magnitude of the SOC pool depends on C inputs to the soil by primary production and C outputs by decomposition (Zhang et al., 2018). Stabilization of SOC links the C input and output, thereby

* Corresponding authors at: Graduate School of Agriculture, Kyoto University, Kyoto 606-8502, Japan (H. Lyu and Tetsuhiro Watanabe).
E-mail addresses: x.lou@live.cn (R. Zhong), lyuhan1993@gmail.com (H. Lyu), watanabe.tetsuhiro.2m@kyoto-u.ac.jp (T. Watanabe).

https://doi.org/10.1016/j.geoderma.2023.116709
Received 11 July 2023; Received in revised form 2 October 2023; Accepted 3 November 2023
Available online 7 November 2023

regulating SOC storage. Various soil properties are recognized as controlling factors for organic matter (OM) mineralization and stabilization. For example, soil pH influences the size, composition, and activity of the microbial community, thereby affecting organic matter mineralization (Cao et al., 2016; Zhou et al., 2019). The pH is also directly associated with the composition of exchangeable cations, especially Ca^{2+} and Mg^{2+}, which stabilize SOC (Lyu et al., 2022; Neina, 2019) via bridging negatively charged mineral surfaces and organic matter (Rowley et al., 2018). The fine-mineral fraction, such as clay, further preserves organic matter by direct (organo-mineral complexes) and indirect (occlusion by aggregation) mechanisms (Rodrigues et al., 2022a). Compared to the fine-mineral fraction content, mineral surface area, closely associated with mineralogy, may be more important for SOC stabilization (Beare et al., 2014; Feng et al., 2011). Active Al/Fe, defined here as the acid-oxalate extractable fraction and composed of poorly crystalline Al/Fe minerals and organo-Al/Fe complexes, was proposed as a more important soil component for SOC preservation in various soil types than fine-mineral fractions, especially acidic soils (Rasmussen et al., 2018; Ashida et al., 2021). The effect of active Al/Fe on carbon stabilization in non-volcanic and neutral-to-alkaline soils is suggested (Rasmussen et al., 2018; Ashida et al., 2021), but its roles are still unclear as their content is generally low (Ashida et al., 2021).

Topsoil and subsoil horizons have large differences in SOC pool size, as well as SOC saturation status (Dai et al., 2022; Lyu et al., 2021b; Possinger et al., 2021). The SOC saturation status, controlled by the relative abundance of soil minerals versus SOC, may regulate SOC stabilization processes and the potential SOC sequestration capacity (Rodrigues et al., 2022b; Yu et al., 2017). Soils with a high level of SOC deficit or a low level of SOC saturation could store a considerable amount of additional SOC (Beare et al., 2014; McNally et al., 2017), particularly in subsoil horizons of cropland soils (Vågen et al., 2005). However, there is limited research on the influence of contrasting SOC saturation conditions in topsoil and subsoil on the mineralization and stabilization of exogenous organic matter. Thus, clarifying the effects of SOC saturation conditions will enhance our ability to manage SOC pools in topsoil and subsoil.

Most studies investigating the influence of exogenous organic matter on SOC pools have either examined organic matter mineralization alone (Rakhsh et al., 2017; Shahbaz et al., 2017; Zhao et al., 2017) or the remaining C in SOM fractions (Rodrigues et al., 2022a; Rodrigues et al., 2022b; Tokarski et al., 2020). Tracing the C in plant residue using ^{13}C-labeled material is a powerful approach for assessing the mineralization of exogenous organic matter (Chen et al., 2019; Zhang et al., 2018). Moreover, SOM fractionation after the incubation of ^{13}C plant material added to soils helps clarify the SOC stabilization mechanisms. Furthermore, the transformation of organic matter molecular composition is rarely examined in soil incubation studies, which is essential in assessing SOC mineralization and stabilization mechanisms. Analytical pyrolysis is a valuable technique for characterizing the molecular composition of bulk SOC, including the identification of biomarkers (Derenne and Quénéa, 2015; Picó and Barceló, 2020). A comparative study at the molecular level using analytical pyrolysis in incubated soils with and without plant-residue addition is warranted to gain a comprehensive understanding of the stabilization mechanisms of exogenous OM in soils.

The Indo-Gangetic Plain (IGP) has a range of climates, from hot, humid monsoon to semi-arid. Massive amounts of clay and silt are transported by rivers like the Ganga and Indus, which are then deposited near the rivers. Soil texture is coarser in upstream (north and west) and finer in downstream (south and east) locations (Pal et al., 2009). As a result, the IGP with its varied climatic zones and gradient of soil properties provides an ideal study region to investigate factors controlling SOC stabilization. Furthermore, SOC content of these soils is very low (4.2 ± 0.9 g kg^{-1}) (Lal, 2004) and may limit agricultural production; however, there may be potential for agricultural management practices to enhance SOC sequestration. Thus, clarification of SOC stabilization potential can benefit practical agricultural activities, as well as increase our mechanistic understanding of SOC stabilization.

This study aims to 1) clarify the roles of soil physicochemical properties (e.g., pH, clay, active Al/Fe and C saturation status) that control the mineralization and stabilization of newly-added plant material to neutral-to-alkaline soils of the IGP; and 2) evaluate the influence of plant material additions on SOM molecular composition by comparing incubated soils with and without maize-addition. We hypothesized that active Al/Fe contributes to SOM stabilization, playing a different role from clay and silt since active Al/Fe content is generally low in near-neutral soils, and that low carbon saturation enhances SOM stabilization due to a more reactive surface. We also expected that analytical pyrolysis would provide further information on stabilized OM. We conducted a 1-year soil incubation with and without addition of ^{13}C-labeled maize using topsoil and subsoil from the upper-to-lower IGP. The objectives were achieved by tracing the maize-derived ^{13}C in respired CO_2 and SOM fractions of the incubated soils. Analytical pyrolysis was conducted at the completion of the incubation to evaluate the influence of maize addition at the molecular level. We anticipated that the wide range of soil properties and SOC saturation conditions in the IGP soils would allow us to elucidate the determinant factors affecting the mineralization and stabilization of soil organic matter.

2. Materials and methods

2.1. Sampling sites and soil samples

Sampling sites (Fig. S1) were chosen across 3 different agro-climatic zones from west-to-east (upper, middle and lower) in the IGP of India. Two locations were chosen within each agro-climatic zone: Meerut (I1) and Kanpur (I2) in the upper, Patna (I3) and Smastipur (I4) in the middle, and Coochbehar (I5) and Canning town (I6) in the lower zones. At each location, soil samples were collected from an agricultural field with the dominant cropping pattern in that area and from an adjacent non-managed secondary forest (Table S1). From west-to-east, elevation decreased (224 → 5 m) and mean annual precipitation increased (840 → 3290 mm) (worldclim.org; (Fick and Hijmans, 2017). Soil temperature regime is hyperthermic, and soil moisture regime is ustic. The soils were formed on mixed alluvium and were classified as Luvisols, Cambisols, and Gleysols according to WRB classification (WRB, 2022) (Table S1). The clay mineralogy of all samples was similar among all sites with a mixture of mica, vermiculite (little hydroxy-Al interlayers), kaolinite and smectite. In detail, soil I3 had a larger amount of smectite, and soil I5 had a higher abundance of chlorite and kaolinite (data not shown).

Soil samples were collected from well-drained soil profiles excavated to a depth of ~ 1 m. While soil samples were collected for each horizon, only the topsoil (0–15 cm) and subsoil (40–60 cm) horizons were used to provide a gradient in SOC concentrations. The 24 samples were divided into 4 groups: forest topsoil (FT), forest subsoils (FS), agricultural topsoil (AT), and agricultural subsoils (AS). All soil samples were air-dried, crushing the large aggregates to pass a 2-mm sieve without pulverizing minerals, and mixed again before analyses.

2.2. Analytical methods

2.2.1. Physicochemical properties

Soil pH was measured in a soil-deionized water suspension (1:5 g/mL) using a pH meter (Benchtop pH meter F-70 Series, Horiba). Exchangeable Ca^{2+}, Mg^{2+}, K^{+}, and Na^{+} were extracted by 1 M NH_4OAc at pH 7.0 and quantified by atomic absorption spectroscopy (Ca^{2+} and Mg^{2+}) and flame emission spectroscopy (K^{+} and Na^{+}) (AA-660, Shimadzu). Then, cation exchange capacity (CEC) was determined by displacement of adsorbed NH_4^+ with 10 % NaCl, using Kjeldahl for NH_4^+ quantification (Soil Survey Laboratory Staff, 1996). Total carbon (TC), nitrogen (TN), and soil organic carbon (SOC) were measured by dry combustion with an EA Isolink CN analyzer (Thermo Fisher Scientific). Calcium carbonate was removed by 0.1 M HCl treatment before

measuring SOC. Inorganic carbon (IC) was determined by difference: IC = TC – SOC. Dissolved organic carbon (DOC) was extracted using 0.5 M K_2SO_4 at a ratio of 1:5 g mL^{-1} and determined by the catalytic oxidation method (TOC-L, Shimadzu, Kyoto, Japan).

For soil particle size analysis, organic matter was removed with boiling H_2O_2, pH adjusted to 9–10, and ultra-sonication for 15 min. The coarse (0.2–2 mm) and fine (0.02–0.2 mm) sand fractions were quantified by wet sieving, whereas the silt (2–20 μm) and clay (<2 μm) fractions were determined by the pipette method (Gee and Or, 2002). Active Al/Fe (Al_o and Fe_o), derived from poorly-crystalline Al and Fe (hydr)oxides and organo-Al/Fe complexes, were extracted with ammonium oxalate solution (0.2 M, pH 3.0) in the dark (4 h) (Blakemore, 1987; Rennert, 2019). Iron in free Fe (hydr)oxides (Fe_d) was extracted in a separate soil aliquot with a combined citrate (0.75 M) and sodium dithionite (1 g in 50 mL) solution (Blakemore, 1987). Extracts were filtered through a 0.45-μm membrane filter and then measured by ICP-AES (ICPE-9000, Shimadzu). The content of crystalline Fe (hydr)oxides was estimated by subtracting Fe_o from Fe_d.

Fine mineral particles (clay + silt, <20 μm) and active Al_o and Fe_o are posited to contribute to SOC stabilization. As an index of SOC saturation, the soil C deficit can be calculated based on SOC and clay + silt contents (Rodrigues et al., 2022a; Stewart et al., 2008), with the protective capacity of clay and silt based on the formula developed by (Stewart et al., 2008):

$$C\ deficit\ = 1\ -\ (SOC/protective\ capacity) \quad (1)$$

$$\text{Protective capacity}_{clay+silt}\left(g\ kg^{-1}\right) = 0.29 \times (clay +\ silt\ content) + 6.9 \quad (2)$$

Similarly, the SOC to active Al_o and Fe_o ratio has a reported maximum value of ~ 30 mol C mol^{-1} $Al_o + Fe_o$ for non-volcanic soils (Ashida et al., 2021). Thus, the protective capacity of active Al_o and Fe_o was calculated as:

$$Protective\ capacity_{Alo+Feo}(\text{cmol}) = 30 \times (Al_o + Fe_o) \quad (3)$$

Furthermore, we used the SOC/(clay + silt) (g g^{-1}) and SOC/(Al_o + Fe_o) (mol mol^{-1}) ratios as simple metrics to estimate the degree of SOC saturation.

2.2.2. Long-term soil incubation with maize addition

We incubated soils with and without the addition of ^{13}C-labeled plant material (12 sites, 2 horizons, 3 replicates, and 2 treatments) to investigate the mineralization and stabilization of organic matter. Firstly, ^{13}C-labeled maize (*Zea mays L.*) (35 % ^{13}C) was grown in a $^{13}CO_2$-rich atmosphere, harvested about one month after germination, and then dried at 70 °C. Maize leaf and stem tissues were ball-milled at 450 rpm for 5 min (PM100, Retsch) (<1 mm) for the incubation experiment. The ground maize (TC: 340 ± 18 g C kg^{-1}, TN: 85 ± 14 g C kg^{-1}) was uniformly mixed into soil samples at a rate of 420 mg C kg^{-1} soil, which is roughly equal to 420 kg C ha^{-1} (assuming a 10-cm depth and bulk density of 1 g cm^{-3}). This amendment amount is similar to the input of post-harvest residues in croplands within the study area (Sukhoveeva, 2022). Twenty grams of each soil sample were prepared with three replications and placed in a sealed glass jar (225 mL, 7-cm diameter). The soil moisture content was adjusted to 55 % of field capacity by adding deionized H_2O. Soil samples were pre-incubated at 25 °C for 7 days prior to the addition of ^{13}C-labeled maize and the start of CO_2 collection (Lyu et al., 2021a; Ma et al., 2021).

The CO_2 released from soils was trapped in a plastic bottle with 10 mL 1 mol/L NaOH trapping solution placed within the incubation jar. Another glass bottle with 0.01 M HCl solution was also placed in the incubation jar to maintain the soil moisture content. Soils were incubated for 364 days and the CO_2-trapping solution was collected at 7, 14, 28, 49, 70, 91, 112, 140, 168, 196, 224, 280, 336 and 364 days for CO_2 quantification. Half (5 mL) of the CO_2-trapping solution was used for determining total CO_2 emission via titration with 0.1 M HCl. The remaining 5 mL of CO_2-trapping solution was used for determining the ^{13}C ratio of the respired CO_2 after treating with $SrCl_2$ to precipitate CO_3^{2-} as $SrCO_3$ (Ma et al., 2021). The ^{13}C ratio of the added maize, the soil sample after incubation, and precipitated $SrCO_3$ were measured with EA-IRMS (EA-IsoLink and DELTA V Advantage, Thermo Fisher Scientific). Replicated standard samples (glucose) were determined at 12-sample intervals to ensure data quality, and the analytical precision for δ^{13}C was ± 0.06 ‰.

The contribution of ^{13}C-labeled maize to total respiration ($Pres_{M\text{-}derived}$) was estimated as follows:

$$Pres_{M-derived} = (atom\%^{13}C_{Mafter} - atom\%^{13}C_{Mbefore})/(atom\%^{13}C_M - atom\%^{13}C_{Mbefore}) \quad (4)$$

where atom%$^{13}C_{Mafter}$, atom%$^{13}C_{Mbefore}$ and atom%$^{13}C_M$ are the ^{13}C atom% of the respired C after maize addition, respired C before maize addition (assumed as ^{13}C atom% of the original soil) and the C of the maize, respectively.

To determine the mineralization rate at an arbitrary date, the mineralization of added maize was fitted to a modified two-pool, first-order kinetic model:

$$C_r = 1 - (a \times e^{-k_a \times t} + b \times e^{-k_b \times t}) \quad (5)$$

where C_r is the ratio of cumulative mineralized carbon to total added carbon amount at time t (days), a and b are the portion of decomposable C pools (a + b = 1) in maize, and k_a and k_b are the rate constants of the C pools. The mineralization rate at each sampling date was calculated by the derivative: $C_r^{'} = a \times k_a \times e^{-k_a \times t} + b \times k_b \times e^{-k_b \times t}$.

2.2.3. Soil organic matter fractionation

Soil organic matter fractionation for soils after incubation was conducted based on previous protocols (Kadono et al., 2008; Lyu et al., 2021a; Paul et al., 2001). Briefly, SOM was fractionated into light (LF) and heavy (HF) fractions using NaI (1.6 g cm^{-3}) density separation. The HF was subsequently dispersed by adding sodium hexametaphosphate and shaking for 15 h for particle size separation: ≥53 μm (occluded particulate organic matter, oPOM) and < 53 μm (mineral-associated organic matter, MAOM). Furthermore, the MAOM was collected to determine the non-hydrolyzable SOM fraction by refluxing with 6 M HCl at 115 °C for 16 h. After measuring the weight of each fraction, total C content was determined by dry combustion.

2.2.4. One-shot Py-GC/MS analysis

After incubation, pyrolysis–gas chromatography–mass spectrometry (Py-GC/MS) was applied to all control and maize-treated soils to evaluate the residual status of added maize after incubation and assess how soil organic compounds were affected by maize addition. Soil samples and maize plant material without ^{13}C labeling were separately ground to a fine powder and homogenized by a ball mill at 450 rpm for 5 min (PM100, Retsch), then dried at 70 °C for 24 h. Analytical pyrolysis was conducted using a multi-functional pyrolyzer (EGA/PY3030D, Frontier Laboratories) coupled with GC/MS (GCMS-QP2020, Shimadzu). A soil sample containing approximately 100 μg C was capsulated (Eco-cup LF, Frontier Laboratories) and pyrolyzed at 550 °C for 1 min. Pyrolysis products were separated in a stainless-steel capillary column (Ultra ALLOY$^+$-5; length = 30 m, internal diameter = 0.25 mm; film = 0.25 μm, Frontier Laboratories). Cryo-trapping (−180 °C) followed by rapid thermal desorption was achieved using a MicroJet Cryo-Trap (MJT-1035E, Frontier Laboratories). The GC oven temperature was held at 50 °C for 1 min and then increased to 300 °C at 10 °C min^{-1}, and stabilized at 300 °C for 5 min (Girona-García et al., 2019). The carrier gas for the whole system was He at a flow rate of 20 mL min^{-1}. Mass detection was activated 1 min later than thermal desorption. The 100 highest peaks for each sample were manually adjusted to reduce baseline noise and interference from nearby peaks, then matched with the

NIST library.

Compounds matched with the reference library (Table S2) were categorized into 15 groups, as listed in Table 2. Each group's proportion was calculated using its chromatogram peak area in the multiple ion chromatogram for *m/z* of 19–500 and the total area of identified compounds. The polysaccharides group represents compounds generated from polysaccharides (e.g., furans), lignin denotes compounds derived from undecomposed lignin (e.g., methoxy phenol), and phenols include phenol and methyl phenols. A group of exclusive compounds for maize was identified by comparing pyrolysis products of non-labeled maize and control soils. Unique compounds exclusive for maize had a relative abundance of > 0.5 % of total identified chromatograph peak areas of the maize material and were not detected in control soil samples. The residual status of maize was evaluated by searching for these compounds in maize-treated soils after incubation.

2.2.5. Statistical analyses

As most parameters (e.g., SOC, exchangeable Ca and Mg, and contents of clay and silt) were not normally distributed and the normality of key parameters even after the log-transformation, Spearman rank correlation coefficients were applied to assess relationships among climate data, soil properties, SOC saturation degree, and organic matter-related properties measured after incubation and SOC fractionation. Bray-Curtis distance-based permutational multivariate analysis of variance (PERMANOVA) was performed to evaluate differences in soil properties between soils from forest and agricultural sites and SOM composition between maize-treated and control soils after incubation (Yan et al., 2021). Nonmetric multidimensional scaling (NMDS) analysis was conducted using the "vegan" and "microeco" packages in R software (Liu et al., 2021; Oksanen et al., 2020). A two-tailed paired *t*-test was applied to assess differences between land uses (forest vs. agriculture) and between horizons (topsoil vs. subsoils). Linear regression was applied to determine numerical relationships between soil properties and the residual C derived from the added maize. Partial least squares path modeling (PLS-PM) was conducted to evaluate the effect of soil properties on stabilization of added maize using "SEMinR" package in R (Hair et al., 2021). Structural model was made based on Spearman correlation matrix. Variance inflation factor (VIF) was used to detect the severity of multicollinearity for factor selection. Bootstrapping PLS-PM was used to provide the significance of path coefficients (β) with confidence intervals. Statistical analyses were performed using R 4.1.1 and IBM SPSS ver. 24.0; significance levels are designated as *, **, and *** for $P < 0.05$, 0.01 and 0.001, respectively.

Table 1
Soil physicochemical properties and selected incubation results for topsoil and subsoil (mean ± standard deviation) and their statistical difference between topsoil and subsoil by paired *t*-test.

	unit	Topsoil	Subsoil	*P* value
pH		7.7 ± 1.1	8.0 ± 1.1	0.259
SOC [a]	g kg^{-1}	13.5 ± 6.6	3.7 ± 0.9	<0.001
DOC	g kg^{-1}	0.19 ± 0.09	0.06 ± 0.02	<0.001
Clay	%	23 ± 13	23 ± 7	0.918
Clay + silt	%	81 ± 15	82 ± 16	0.555
$Ca_{ex} + Mg^a_{ex}$	$cmol_c$ kg^{-1}	16 ± 12	14 ± 10	0.526
$Na_{ex} + K^a_{ex}$	$cmol_c$ kg^{-1}	0.6 ± 0.3	0.5 ± 0.3	0.112
$Al_o + Fe_o$ [a]	cmol kg^{-1}	6.2 ± 4.0	5.1 ± 2.6	0.142
Al_o	cmol kg^{-1}	2.2 ± 1.3	2.1 ± 0.7	0.508
Fe^a_d	cmol kg^{-1}	14.3 ± 6.0	18.5 ± 9.2	0.023
$Fe_d - Fe_o$	cmol kg^{-1}	10.4 ± 4.1	15.4 ± 7.8	0.002
SOC/(clay + silt)	g g^{-1}	0.017 ± 0.009	0.005 ± 0.001	0.001
$SOC/(Al_o + Fe_o)$	mol mol^{-1}	25.5 ± 18.8	7.3 ± 3.3	0.004
C $deficit_{clay + silt}$ [b]	%	56 ± 22	87 ± 5	0.001
C $deficit_{Alo + Feo}$ [b]	%	16 ± 74	74 ± 11	0.004
M_Maize [c]	mg C kg^{-1}	215 ± 24	186 ± 29	0.003
M_Soil [c]	mg C kg^{-1}	1048 ± 366	390 ± 178	<0.001
M_Total [c]	mg C kg^{-1}	1263 ± 369	576 ± 190	<0.001
R_Maize [c]	mg C kg^{-1}	143 ± 28	160 ± 40	0.073
LF_M [c]	mg C kg^{-1}	24 ± 33	24 ± 18	0.985
HF_M [c]	mg C kg^{-1}	116 ± 28	136 ± 15	0.033
oPOM_M [c]	mg C kg^{-1}	11 ± 10	13 ± 8	0.094
MAOM_M [c]	mg C kg^{-1}	101 ± 20	104 ± 14	0.661

[a] SOC, soil organic carbon; DOC, dissolved organic carbon; $Al_o + Fe_o$, active Al and Fe extracted by acid oxalate solution; $Fe_d - Fe_o$, crystalline free iron (hydr) oxides; Ca_{ex}, Mg_{ex}, Na_{ex}, K_{ex}, exchangeable Ca^{2+}, Mg^{2+}, Na^+, K^+;

[b] C $deficit_{clay + silt}$, C deficit index calculated based on SOC and clay + silt contents; C $deficit_{Alo + Feo}$, C deficit index based on SOC and active Al and Fe contents.

[c] M_Maize, mineralized maize-derived C; M_Soil, mineralized original SOC; M_Total, sum of mineralized maize-derived C and SOC; R_Maize, residual maize-derived C in soil; LF_M, maize-derived C in light fraction; HF_M, maize-derived C in heavy fraction; oPOM_M, maize-derived C as occluded particulate organic matter in aggregates; MAOM_M, maize-derived C as mineral-associated organic matter.

Table 2
Relative abundance of organic compounds (mean ± standard deviation, n = 24) in maize-treated and control soils at the end of the incubation period and their statistical difference between maize-treated and control soils by *t*-test.

Name	Mean abundance in maize-treated soil	Mean abundance in control soil	*P* value
	%	%	
Polysaccharides	10.2 ± 7.0	8.8 ± 4.0	0.115
Long alkanes [a]	2.6 ± 1.7	1.8 ± 1.8	0.147
Short alkanes [a]	2.0 ± 0.9	1.3 ± 0.9	0.007
n-alkenes	3.3 ± 1.9	1.8 ± 1.0	<0.001
Squalene	3.8 ± 6.3	2.3 ± 3.8	0.285
FAnE [a]	17.9 ± 17.2	4.9 ± 6.6	<0.001
Steroids	0.9 ± 1.2	1.7 ± 5.0	0.371
Lignin	0.5 ± 0.6	0.5 ± 0.9	0.918
Phenols	3.1 ± 3.2	1.9 ± 2.4	0.003
MAH [a]	11.4 ± 4.2	17.0 ± 9.7	0.028
PAH [a]	1.5 ± 0.9	1.5 ± 1.2	0.868
N-MAH [a]	2.0 ± 1.1	2.2 ± 1.0	0.199
Alkylamides	0.3 ± 0.5	0.4 ± 0.5	0.688
N-containing [a]	39.3 ± 15.2	52.5 ± 17.8	0.005
Other hydrocarbons	1.2 ± 1.2	1.3 ± 1.5	0.795
Total	66 ± 11	68 ± 16	0.507

[a] long alkanes (C23 to C33); short alkanes (C7 to C22); FAnE, fatty acids and their esters; MAH, monocyclic aromatic hydrocarbons; PAH, polycyclic aromatic hydrocarbons; N-MAH, N-containing MAH; N-containing, non-aromatic N containing compounds.

3. Results

3.1. Physicochemical properties

The physicochemical properties of soils at each sampling location are summarized in Table S3. In general, the soil of forest versus agriculture sites had few significant differences in soil properties as inferred from PERMANOVA (Fig. S2). Significant differences between forest and agriculture soils were only found in Fe_d and C-$deficit_{Alo + Feo}$, which were lower in the forest versus agriculture soils. Soil pH (H_2O) ranges for FT, FS, AT and AS were 6.4–8.8, 6.0–9.2, 6.2–9.9, and 5.7–9.0, respectively. Most of the soils had near-neutral to alkaline pH values, which gradually decreased from the upper to lower IGP (Fig. S3) as precipitation/leaching increased. High IC contents were found in soils from I4 (Table S3), which included many carbonate shells in the sand fraction. The contents ($cmol_c$ kg^{-1}) of exchangeable Na^+ (0.29 ± 0.25) and K^+ (0.21 ± 0.21) were much lower than exchangeable Ca^{2+} (11.7 ± 10.4) and Mg^{2+} (3.3 ± 3.0), revealing their limited bio-toxicity.

Active Al and Fe ($Al_o + Fe_o$) content was very low (<14 cmol kg^{-1}) across all sites. The $Al_o + Fe_o$, clay, and clay + silt in topsoil horizons were similar to those in subsoil horizons (Table 1). From the upper to lower IGP, $Al_o + Fe_o$ content increased gradually and was positively correlated with MAP ($r_s = 0.58$**) and negatively correlated with soil pH ($r_s = -0.67$***) (Fig. S4). Free Fe (hydr)oxides (Fe_d) and crystalline Fe

(hydr)oxides ($Fe_d - Fe_o$) were higher in subsoil horizons (Table 1). Fe_d positively correlated with Fe_o and $Al_o + Fe_o$ (Fig. S4). Clay and clay + silt content increased from the upper to lower IPG, ranging from 10 to 59 % and 45 to 100 % (Table S3, Fig. S5). Most soil textures were silty loam, whereas a few samples from the lower IGP were silty clay loam to clay (Table S3, Fig. S5). CEC ranged from 4.7 to 23.3 $cmol_c\ kg^{-1}$ and increased with clay content ($r_s = 0.73$***), but not with SOC (Fig. S4).

SOC and DOC of topsoil were significantly higher than subsoils across all sites (Table 1, Fig. S6a). DOC was positively correlated to SOC and negatively correlated to $Fe_d - Fe_o$ (Fig. S4). C-$deficit_{clay\ +\ silt}$ displayed a negative correlation with SOC/(clay + silt) ($r_s > -0.99$***), as did C-$deficit_{Alo\ +\ Feo}$ and SOC/($Al_o + Fe_o$) ($r_s > -0.99$***, Fig. S4). SOC/(clay + silt) and SOC/($Al_o + Fe_o$) were significantly higher, and C-$deficit_{clay\ +\ silt}$ and C-$deficit_{Alo\ +\ Feo}$ were significantly lower in topsoil than subsoil horizons (Table 1). As C deficits (i.e., C-$deficit_{clay+silt}$ and C-$deficit_{Alo+Feo}$) and carbon saturation indices (i.e., SOC/(clay + silt) and SOC/($Al_o + Fe_o$)) displayed identical trends, we applied SOC/(clay + silt) and SOC/($Al_o + Fe_o$) to simplify the subsequent discussion.

3.2. Long-term soil incubations

Mineralization of the added ^{13}C-labeled maize predominantly occurred during the first 70 days and dropped to very low levels by day 336 (Fig. 1), whereas mineralization of the SOC continued throughout the entire incubation period. The total recovery of ^{13}C from the added maize (i.e., CO_2 trapped in alkaline solution + remaining in soil) was 84 ± 7%. The mean mineralized C from maize was 215 mg C kg^{-1} for topsoils and 186 mg C kg^{-1} for subsoils, corresponding to 51 ± 6% and 44 ± 7% of the added maize in topsoil and subsoil horizons, respectively.

Mineralization rates of the added maize slowed as the incubation proceeded (Fig. 1) and was most rapid in the first 28 days. Mineralization rates of the added maize on the 7th day (0.13 to 0.52 mg C day^{-1} $sample^{-1}$) were significantly correlated with SOC ($r_s = 0.50$*) and Al_o ($r_s = -0.53$**), and the mineralization rates on the 14th and 28th days (0.01 to 0.52 mg C day^{-1} $sample^{-1}$) were negatively correlated with Al_o ($r_s = -0.64$*** and -0.50*) and Fe_o ($r_s = -0.43$* and -0.49*), and positively correlated with pH ($r_s = 0.45$* and 0.52**) (Fig. 2 and S7). Mineralization rates in the later stages (after 28th days) gradually decreased till the end of the incubation (decreased from 0.01 to less than 8×10^{-3} mg C day^{-1} $sample^{-1}$). Mineralization rates after 70th days were positively correlated with SOC, DOC, and SOC/($Al_o + Fe_o$), and negatively correlated with $Fe_d - Fe_o$. For instance, the correlation coefficients for the mineralization rate versus SOC/($Al_o + Fe_o$) at the 91st and 364th days were 0.63*** and 0.62**, respectively (Fig. S8). After the 91st day, the mineralization of added maize was very low ($<8 \times 10^{-3}$ mg C day^{-1} $sample^{-1}$), especially for subsoil horizons ($3.1 \pm 1.3 \times 10^{-3}$ mg C day^{-1} $sample^{-1}$) (Fig. S8).

Mineralized C derived from maize in topsoil horizons was significantly higher than in subsoil horizons. The amount of mineralized maize tended to decrease from the upper to lower IGP, especially for topsoil horizons (Fig. S9). Mineralized C from added maize displayed an increasing trend with increasing soil pH (Fig. S10a) and was positively correlated with SOC/($Al_o + Fe_o$) ($r_s = 0.53$**). The mineralized C from maize reached maximum values at a SOC to $Al_o + Fe_o$ molar ratio of 15 or larger (Fig. S10b).

Residual maize C in topsoil and subsoil horizons was 143 ± 28 mg C kg^{-1} and 160 ± 40 mg C kg^{-1}, respectively (Table 1). The residual maize C was positively correlated with clay ($r_s = 0.45$*), clay + silt ($r_s = 0.48$*), and $Al_o + Fe_o$ ($r_s = 0.46$*) across all sites (Fig. 3). Moreover, the

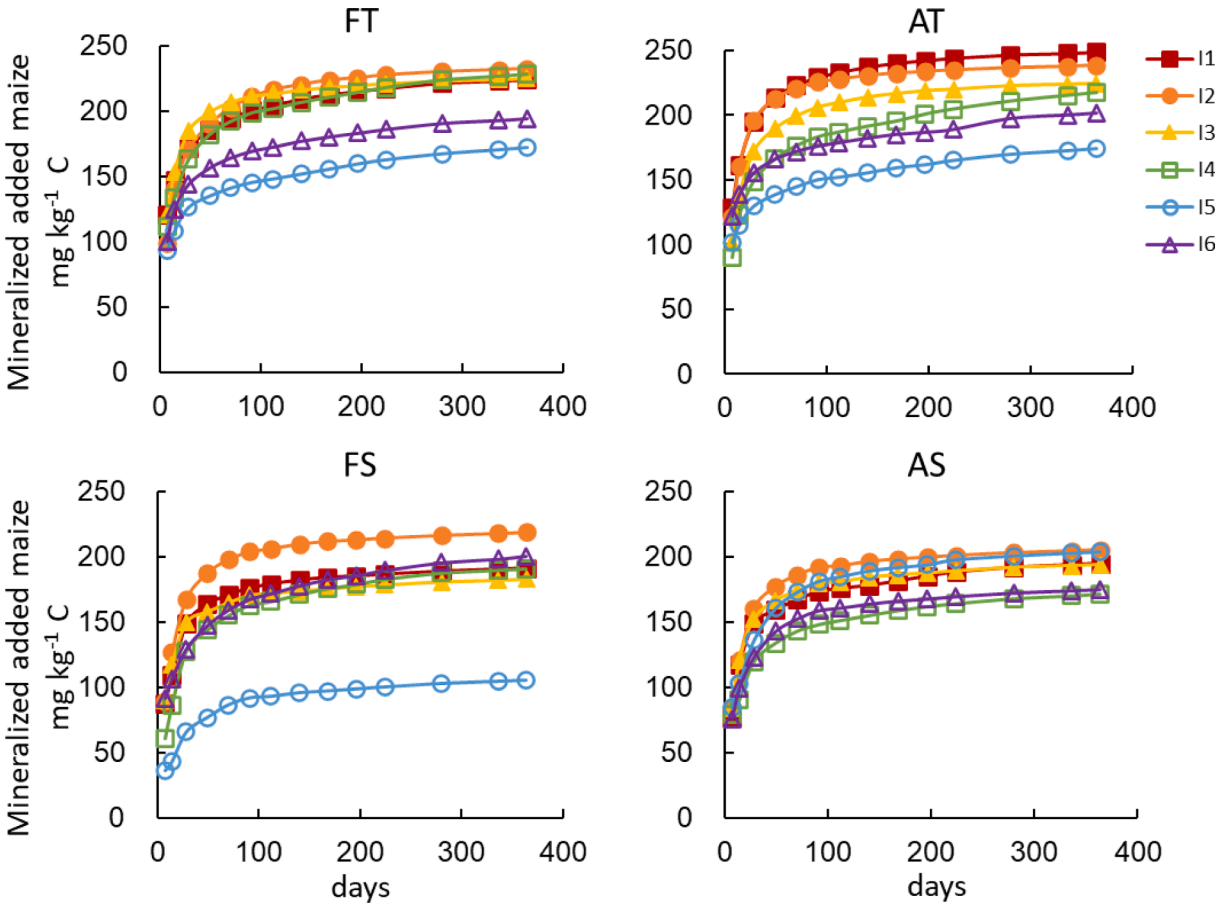

Fig. 1. Cumulative mineralized maize-derived C. FT, FS, AT, AS, forest topsoil, forest subsoil, agriculture topsoil, agriculture subsoil, respectively; I1 and I2 are located in the upper, I3 and I4 in the middle, and I5 and I6 in the lower agro-climatic zones of IGP.

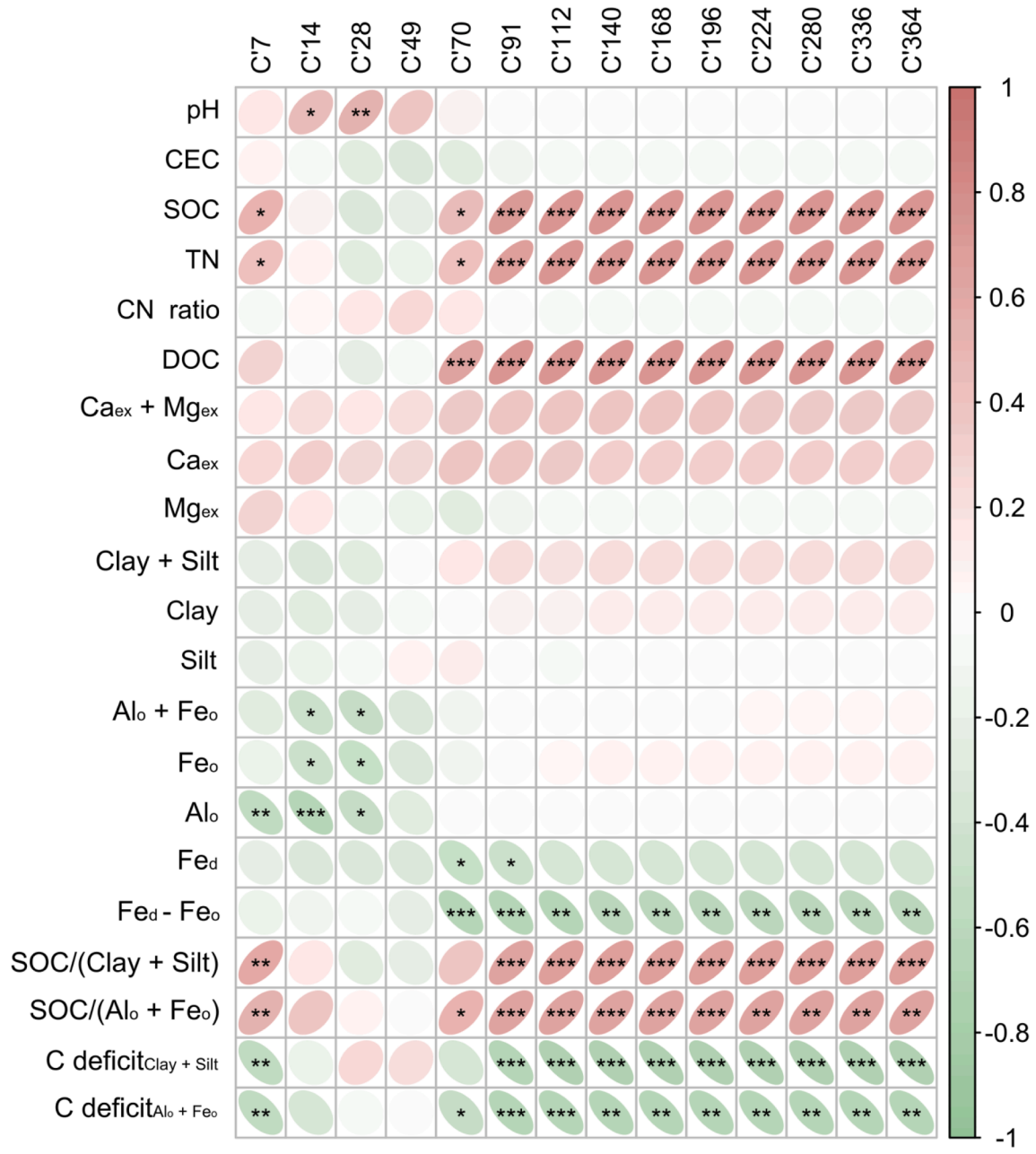

Fig. 2. Spearman correlation matrix (r_s) between soil physicochemical properties and mineralization rate of added maize on different days. C'7 to C'364, the respiration rate of each sampling date. The green and red symbols represent the correlation coefficient of each paired property, as indicated by the bar on the right-hand side. The shape of symbols changes from a perfect circle to a straight line: a perfect circle of the colored symbols indicates a correlation coefficient of 0, and a straight line indicates a correlation coefficient of 1 or −1. CEC, cation exchange capacity; SOC, soil organic carbon content; TN, total nitrogen content; DOC, dissolved organic carbon; Ca_{ex}, exchangeable calcium; Mg_{ex}, exchangeable magnesium; $Al_o + Fe_o$, oxalate-extractable aluminum plus iron; Fe_d, dithionite-citrate extractable iron; $Fe_d - Fe_o$, crystalline free iron (hydr)oxides; C $deficit_{Clay + Silt}$, C deficit estimated based on SOC and clay + silt contents; C $deficit_{Alo + Feo}$, C deficit estimated based on SOC and oxalate-extractable aluminum and iron. *, **, and *** indicate significance at $P < 0.05$, 0.01 and 0.001, respectively.

intercept of regression formulas for the residual maize C versus clay content and $Al_o + Fe_o$ were ~ 120 mg C kg^{-1} (Intercept = 114** and 123**, respectively) (Figs. S10cd).

3.3. SOM fractionation

The amount of maize-derived C in different SOM fractions is shown in Fig. 4. More than 70 % of residual maize-derived C was in relatively stable fractions, except for I5-FT (54 %), that is, OM occluded in aggregates (oPOM, 8 ± 4 %) and associated with minerals (MAOM, 77 ± 15 %) (Fig. 4). Maize-derived C in HF was significantly higher in subsoil than topsoil horizons. Across sampling locations, lower IGP sites had the highest residual maize-derived C in both topsoil and subsoil horizons. Similarly, the amount of maize-derived C in LF and oPOM was higher in lower IGP sites (Fig. 4).

There was a significant negative correlation between the amount of maize-derived C in LF and pH ($r_s = -0.46$*) (Fig. S12a). The maize-derived C in oPOM displayed correlations with pH ($r_s = -0.63$**), clay + silt ($r_s = 0.64$***), $Al_o + Fe_o$ ($r_s = 0.78$***), and SOC/($Al_o + Fe_o$) ($r_s = -0.61$**) (Figs. 3, S12b, S13). Also, maize-derived C in MAOM had a positive correlation with clay content ($r_s = 0.77$***). These correlations related to maize-derived C in oPOM and MAOM were found even

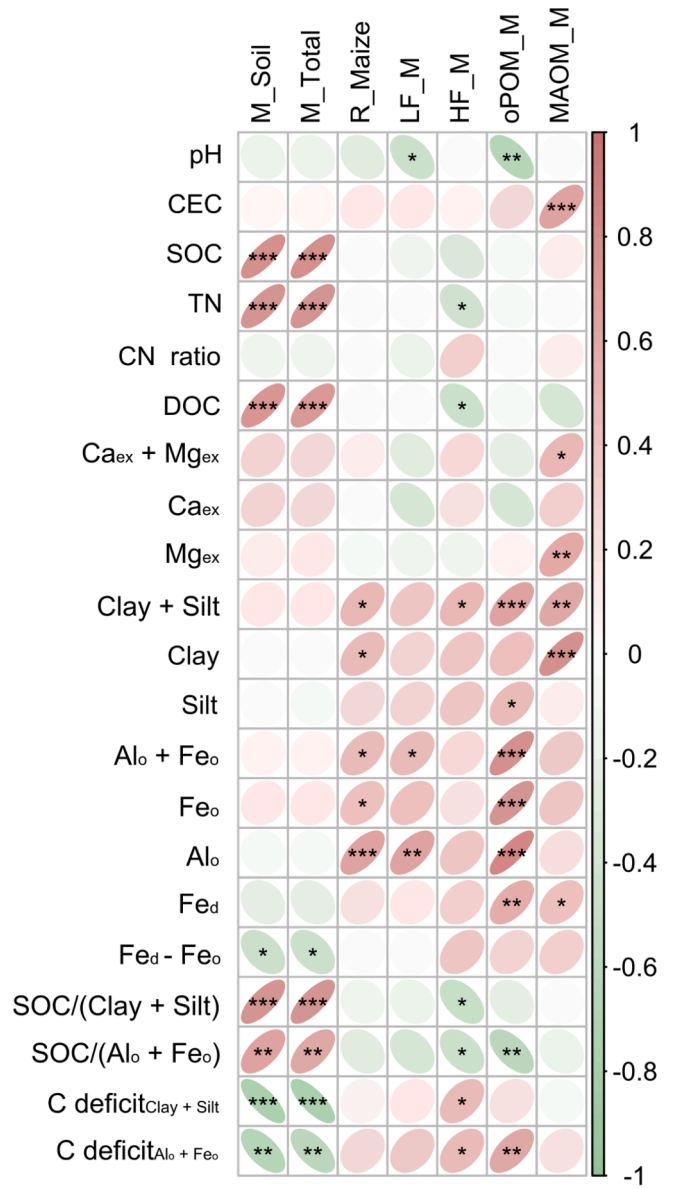

Fig. 3. Spearman correlation matrix (r_s) between soil physicochemical properties and selected incubation results across all soils. The green and red symbols represent the correlation coefficients of each paired property, as indicated by the bar on the right-hand side. The shape of symbols changes from a perfect circle to a straight line: a perfect circle indicates a correlation coefficient of 0, and a straight line indicates a correlation coefficient of 1 or −1 M_Soil, mineralized original SOC; M_Total, sum of mineralized maize-derived C and SOC; R_Maize, remaining maize-derived C; LF_M, maize-derived C in light fraction; HF_M, maize-derived C in heavy fraction; oPOM_M, maize-derived C as occluded particulate organic matter in aggregates; MAOM_M, maize-derived C as mineral-associated organic matter. CEC, cation exchange capacity; SOC, soil organic carbon; TN, total nitrogen; DOC, dissolved organic carbon; Ca_{ex}, exchangeable calcium; Mg_{ex}, exchangeable magnesium; $Al_o + Fe_o$, oxalate-extractable aluminum plus iron; Fe_d, dithionite-citrate extractable iron; $Fe_d - Fe_o$, crystalline free iron (hydr)oxides; C $deficit_{Clay + Silt}$, C deficit estimated based on SOC and clay + silt contents; C $deficit_{Alo + Feo}$, C deficit estimated based on SOC and oxalate-extractable aluminum and iron.*, **, and *** indicate significance at $P < 0.05$, 0.01 and 0.001, respectively.

when topsoil and subsoil horizons were separately analyzed (Fig. S11).

Partial least squares path modelling (PLS-PM) was utilized to evaluate the contribution of soil properties, which were influenced by climate, river (lower basin has finer particles), and soil horizon, on stabilization of added maize (Fig. 5). Maize-derived C in oPOM was well explained ($r^2 = 0.56$) with direct contribution by $Al_o + Fe_o$ ($\beta = 0.62$***) and SOC/($Al_o + Fe_o$) ($\beta = -0.22$*). Clay plus silt indirectly contributed to maize-derived C in oPOM by cooperating with $Al_o + Fe_o$ ($\beta = 0.46$*). Maize-derived C in MAOM was also well explained ($r^2 = 0.74$) and was only directly and positively contributed by clay content ($\beta = 0.81$**), which was more abundant in lower IGP. The contributions of CEC and exchangeable Ca and Mg to both maize-derived C in oPOM and MAOM were not significant in the model.

3.4. Py-GC/MS analyses

A total of 15 unique compounds (peaks) specific to maize plant material (23 % of total identified peak area) was found when comparing the Py-GC/MS chromatographs of maize (Fig. S14) with the control soils. Those peaks had a relative abundance of > 0.5 % in the chromatograph for maize material but were not present in the 24 control soils (Table S4). Of the 15 unique peaks identified for maize plant materials, we found only two of these peaks, namely 2-cyclopenten-1-one and 2-methoxy-4-vinylphenol in the maize-incubated soils (Table S5). The 2-cyclopenten-1-one is derived from polysaccharides (Buurman et al., 2007; Chen et al., 2018), and 2-methoxy-4-vinylphenol is derived from partially-degraded lignin (Ansari et al., 2019; Nakagawa-Izumi et al., 2017). None of the 15 unique maize peaks were found for most of the maize-incubated soils (18 of 24 soils). For instance, pyrolysis products of lignocellulose and cellulose, such as acetol, 2-hydroxy-3-methyl-2-cyclopenten-1-one and 3-ethyl-2-hydroxy-2-cyclopenten-1-one- (Ansari et al., 2019; Wang et al., 2012), were not found in maize-incubated soils. Also, peaks of plant metabolites and steroids from maize, such as phytol, vitamin E and beta-sitosterol acetate were absent (Ahn et al., 2016) (Tables S2 and S4).

The effects of maize material treatment on organic matter composition were evaluated by comparing the maize-treated and control soils after incubation (Table 2, Fig. S15). About 67 % of pyrolysis peaks (66 ± 11 % for treatment soils and 68 ± 16 % for control soils) were quantified and categorized into 15 compound groups, while the remaining 33 % were mostly small molecules (e.g., butene) that were not attributable to the original organic compounds before pyrolysis. As an example, pyrolysis peaks of I5 are shown in Fig. S17. The majority of lignin-derived compounds in maize, 2-methoxy-4-vinylphenol (42 % of maize lignin) and 2-methoxy-phenol (47 % of maize lignin) were not found in subsoil horizons. However, four (2-methoxy-phenol found in I4-FT, I5-AT, I6-FT and I6-AT; Table S5) and six (2-methoxy-phenol found in I1-FT, I1-AT, I2-FT, I4-FT, I6-FT and I6-AT) topsoils did contain lignin-derived compounds. In those topsoil horizons, 2-methoxy-4-vinylphenol and 2-methoxy-phenol proportions were significantly higher in the maize-incubated than in control soils ($P < 0.05$).

A significant difference in SOM composition between the maize-treated and the control soils after incubation was identified using NMDS ordination and PERMANOVA testing (Fig. S16). As decomposition products of lignin, phenols (i.e., phenol and alkylphenol) were significantly higher in soils with maize addition across all sites and horizons (Table 2, Fig. S15). A predominant difference was soils with maize addition had a significantly higher proportion of FAnE than control soils (Table 2, Fig. S17). The increase of FAnE in maize-incubated soils was mainly due to the increase of n-hexadecanoic acid and octadecanoic acid, which are the main components or derivatives of fatty acids and their esters in maize plant materials. Short alkanes and n-alkenes were also higher in the maize-incubated soils than in the controls (Table 2). In contrast, N-containing non-aromatic hydrocarbons (N-containing) were significantly lower in the maize-incubated soils (Table 2, Figs. S15 and S17). The effects of maize addition on the increased FAnE and decreased N-containing components were more evident in subsoil horizons (Fig. S15).

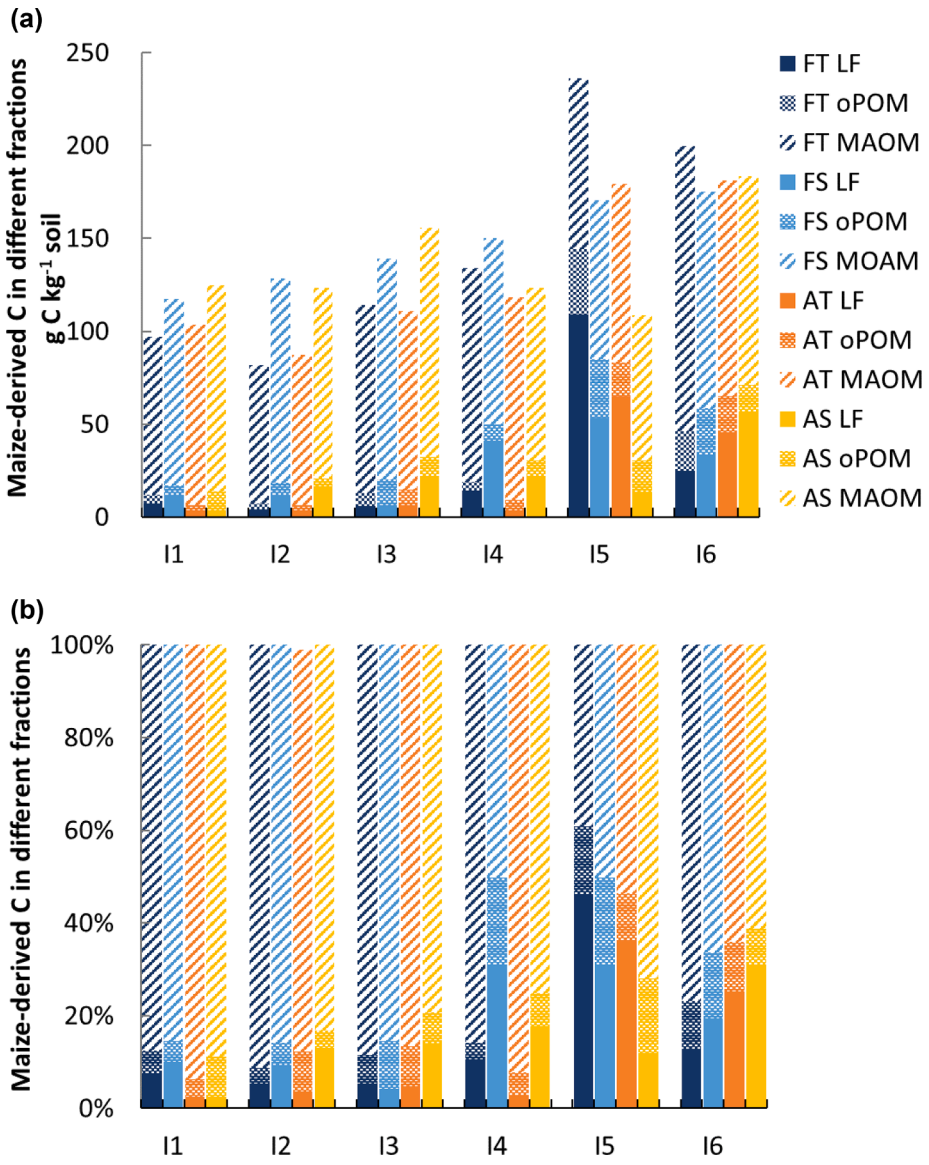

Fig. 4. Content of maize-derived C in soil (a) and proportion of maize-derived C in different SOM fractions (b) after one-year incubation. FT, FS, AT, AS, forest topsoil, forest subsoil, agriculture topsoil, agriculture subsoil, respectively; LF, light fraction; oPOM, occluded particulate organic matter in aggregates; MAOM, maize-derived C as mineral-associated organic matter; I1 and I2 are located in the upper, I3 and I4 in the middle, and I5 and I6 in the lower agro-climatic zones of IGP.

4. Discussion

4.1. Factors regulating mineralization of maize plant material

Soil pH, $Al_o + Fe_o$, SOC and degree of SOC saturation were identified as the primary factors regulating the mineralization rate of added maize. Because soil properties between the forest and agriculture sites were similar (Fig. S2) and showed similar trends in mineralization and stabilization of the added maize, the results from the two land-use types were combined in the following discussion. The rapid mineralization of maize during the first 70 days (Fig. 1) corresponds to the primary decomposition stage (Trinsoutrot et al., 2000). First-week mineralization rates of the added maize were negatively correlated with Al_o, and positively correlated with original SOC content and SOC saturation degree (SOC/($Al_o + Fe_o$) & SOC/(clay + silt)) (Fig. 2). Aggregation can occur quickly during wet-dry cycles and/or physical disturbance events (Oades and Waters, 1991; Tisdall, 2020), which is similar to the process of rewetting and maize incorporation at the beginning of the incubation. Although the absolute values of active Al/Fe are considered low compared to acidic soils, they appear to be highly effective binding agents active in formation of soil aggregates (Wagai et al., 2020). Initially formed aggregates may break down in later incubation stages (i.e., after day 196) and release some of the occluded maize for microbial utilization. Alternatively, some of these aggregates are likely reinforced by microbially generated organic materials derived from maize, thereby contributing to OM occlusion within aggregates (Beare et al., 1994; Coleman et al., 2018; Feller and Beare, 1997) (Fig. 3). The correlation between mineralization rate and Al_o, rather than Fe_o (or Fe_d) (Fig. 2 and S7), may result from Al being more soluble than Fe across a wide range of pH values rendering it more interactive with organic matter (Ashida et al., 2021).

A higher microbial energy supply from soils with higher SOC can support a more active microbial community with a larger abundance of copiotroph microbes (Koch, 2001), which were previously demonstrated to have a strong response to organic matter additions (Dungait et al., 2011; Wu et al., 2020). Higher carbon saturation degrees/lower carbon deficits indicate that a larger proportion of the stabilization capacity is filled, thereby decreasing its ability to stabilize additional SOC

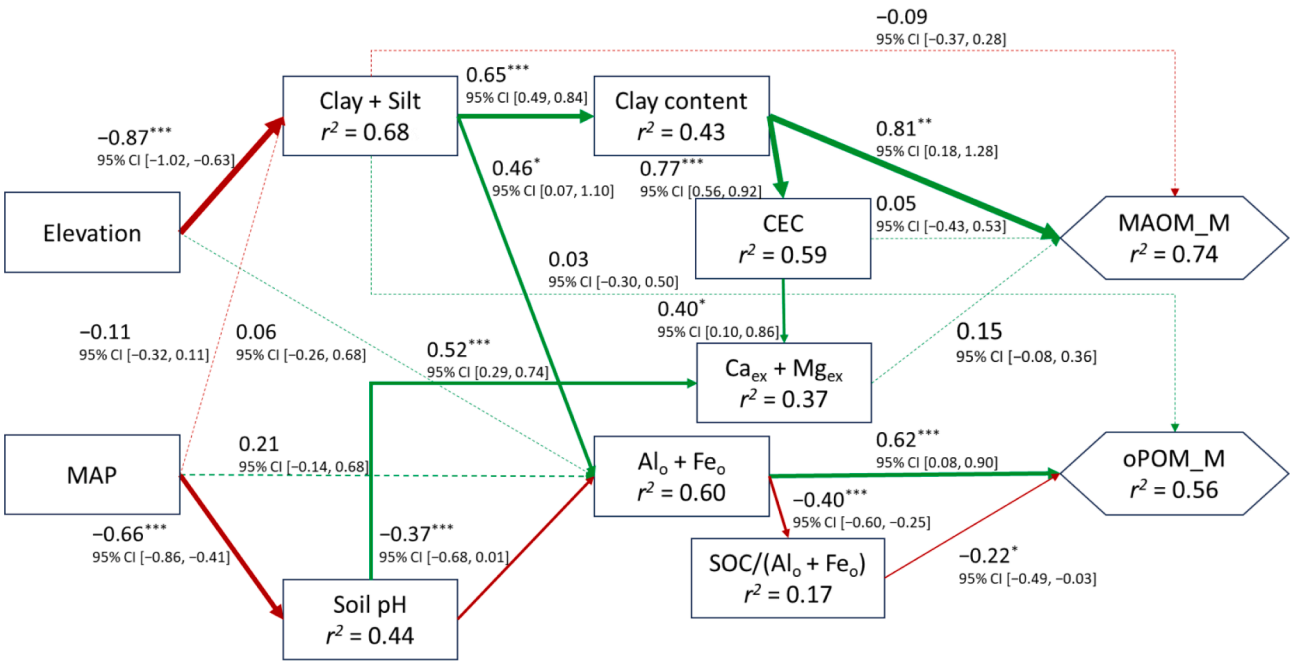

Fig. 5. Partial Least Squares Path Modeling (PLS-PM) for evaluating the effect of soil properties on the stabilization of added maize. MAP, mean annual precipitation; Ca_{ex} + Mg_{ex}, exchangeable calcium plus magnesium; Al_o + Fe_o, oxalate-extractable aluminum plus iron; CEC, cation exchange capacity; MAOM_M, maize-derived C as mineral-associated organic matter; oPOM_M, maize-derived C as occluded particulate organic matter in aggregates. Solid and dotted arrows represent the significant and non-significant contributions, respectively; green and red colors represent the positive and negative contributions, respectively; the number above the arrow line represents the normalized path coefficient (β). The significance of each path coefficient and the confidence interval (CI) of the path coefficient were provided by model bootstrapping.

(McNally et al., 2018; Rodrigues et al., 2022b) and leading to greater microbial respiration. A higher microbial activity/respiration occurred in soils with higher SOC, DOC, and higher SOC saturation as demonstrated by their strong positive correlations. This resulted in a greater amount of mineralized C from the original SOC, as well as the total mineralized C (i.e., C from original SOC + added maize) (Fig. 3).

After initiation of maize mineralization by quick-response microbes, decomposition of maize during later incubation stages appears to be influenced by pH-regulated enzyme activities, as well as the stabilization of maize material (probably both aggregation and direct stabilization) by Al_o (and Fe_o) (Figs. 2 and S7). The ability of active Al and Fe to immobilize extracellular enzymes (Allison, 2006; Koji, 1989) may also retard the decomposition of organic matter with high-molecular-weight compounds in fresh plant material. Higher pH in drier upper IGP can make some components of the added maize more soluble (Curtin et al., 2016), with the DOM being more accessible to microbes (Figs. 2 and 3). Additionally, utilization and decomposition of fresh plant materials, such as lignin and fatty acid esters, require the production of extracellular enzymes (i.e., laccase and acetylesterase) (Perez et al., 2002) that are more effective at near-neutral pH values (Fujii et al., 2020; Puissant et al., 2019). Hence, we posit that the positive correlations between mineralization rates on the 14th and 28th days and soil pH demonstrate that a higher pH promotes the decomposition of plant material by enhancing enzyme activities (Figs. 2 and S7).

Once the increase in total respiration due to maize addition settled after 70 days of incubation, the original SOC, DOC, and SOC saturation degree appear to regain control of the mineralization rate for added maize. The positive correlations between the mineralization rates of added maize and indices of carbon saturation after 70 days (Figs. 2 and S8) infer that soils with lower SOC saturation have greater SOC stabilization by active Al/Fe and crystalline clay minerals (Kleber et al., 2007; Lyu et al., 2021a; Stewart et al., 2008). These stabilization processes can preserve decomposition products from the primary decomposition stage, thereby retarding further mineralization. For soils with high SOC and DOC, continued high mineralization rates after 70 days of incubation may suggest a more limited stimulus by the maize addition (i.e., 420 mg C kg^{-1} soil for maize addition) as the maize addition did not permanently change the microbial community (Blagodatskaya and Kuzyakov, 2008; Kuzyakov, 2010). After stabilization of respiration rates (Fig. 1), energy from the original SOC and primary decomposition products weakly associated with soil minerals, as suggested by the higher SOC saturation degrees, can cause higher microbial activity and associated higher mineralization rates. Moreover, higher mineralization rates for maize-derived C occurred in topsoil horizons with higher SOC contents and higher SOC saturation degrees (Fig. S8) than subsoil horizons during the later incubation stage. This further suggests that differences in the original SOC and SOC saturation degrees could regulate organic matter mineralization by controlling microbial activities through substrate accessibility/availability.

4.2. Factors controlling SOC stabilization and fates of maize-derived C

Active Al/Fe and fine mineral particles promoted the accumulation of maize-derived C as inferred by the positive correlations of residual maize-derived C with Al_o, Fe_o and clay (+silt) (Figs. 3 and S10). Because carbon-use efficiency by microbes is about 0.4–0.7 (Manzoni et al., 2012; Saifuddin et al., 2019), the 48 ± 7 % of cumulative maize mineralization (Fig. 1, Table 1) suggests that most of the added maize was processed by microorganisms. Higher clay (+silt) content and Al_o (+Fe_o) (Table S3) in the lower IGP sites appear to have contributed to greater stabilization of microbially processed C from the added maize (Fig. 5). Interestingly, the stronger correlation between remaining maize content and Al_o suggests that Al_o might be more effective at stabilizing OM compared to Fe_o (Fig. 3). The lower amount of stabilized maize-derived C in topsoil horizons (Fig. 4a) is ascribed to less efficient stabilization of OM in topsoil versus subsoil horizons due to its higher SOC saturation degree (Fig. S6, Table 1). The positive correlation between cumulative mineralization of maize and SOC/(Al_o + Fe_o) and the limited release of CO_2 derived from maize after one year of incubation indicate that the SOC saturation degree may be important in controlling the

mineralization of added organic matter (McNally et al., 2018; McNally et al., 2017), consistent with our second hypothesis. Under lower SOC saturation conditions, organic matter is more strongly stabilized by soil minerals via inner sphere interactions (Kleber et al., 2007), which attenuates further organic matter decomposition. Notably, the OM stabilization capacity seems to have a limit, as the mineralized maize-derived C reached a threshold when the ratio of SOC to $Al_o + Fe_o$ reached ~ 15 (Fig. S10b).

Because the active Al/Fe (5.6 ± 1.0 cmol kg^{-1}) and Fe_d (16.4 ± 7.9 cmol kg^{-1}) contents were low, OM stabilization by direct adsorption or complexation with active Al/Fe or Fe (hydr)oxides is expected to play only a minor role. Moreover, the non-zero intercepts for plots of mineralized C with active Al/Fe and clay (Figs. S10cd) imply that even without clay minerals or active Al/Fe present, the added maize would not completely mineralize within a year. This suggests that the accumulation of added maize in the soil is not totally dependent on clay or active Al/Fe contents. For instance, soil pH (Fig. S10a), recalcitrance of some organic maize components (e.g., lignin), and microbial accessibility may also limit mineralization (Dungait et al., 2012; Marschner et al., 2008; Rousk et al., 2009). As the total mineralization of added maize was close to 50 % and further release of maize-derived CO_2 was nearly undetectable after 336 days (Fig. 1), the residual maize-derived C was considered predominantly stabilized (West and Marland, 2003). Hence, fractionation of organic C after incubation was investigated further to assess stabilization mechanisms for the residual maize-derived C.

Based on SOM fractionation, maize-derived C was mainly stabilized by soil minerals (i.e., clay, silt, and active Al/Fe) and preserved as MAOM and oPOM (Fig. 4). The MAOM fraction was the major destination of maize-derived C (77 ± 15 % of residual maize C), which is controlled primarily by clay. Because of the similar clay mineralogy among all sites, the difference in clay mineral surface area caused by mineralogy variation can be ignored. The predominant contribution of clay content to maize-derived MAOM ($\beta = 0.81$**; Fig. 5) infers that clay minerals controls the majority of organic matter stabilization. The negative charge provided by clay minerals (e.g., vermiculite) can contribute to the preservation of organic matter as MAOM by adsorbing polar or charged functional groups (Kleber et al., 2007). This premise is further supported by the significant positive correlation between CEC and maize-derived MAOM ($r_s = 0.64$***). Multivalent exchangeable Ca^{2+} and Mg^{2+} (Fig. 3), which were more abundant in the higher pH soils of drier upper-to-middle IGP (Table 1, Fig. 5), can provide a bridge connecting the negatively charged mineral surfaces and organic matter (Rowley et al., 2018), thereby stabilizing the added organic matter from microbial utilization. However, this bridging effect seemed not predominant in stabilizing added maize as MAOM, as revealed by its insignificant contribution to maize-derived MAOM ($\beta = 0.15$; Fig. 5). On the other hand, maize-derived MAOM had no clear relationship with active Al/Fe, which may be due to their very low contents in the IGP soils, as compared to volcanic soils (Garrido and Matus, 2012; Lyu et al., 2022; Ugolini and Dahlgren, 2002) and acidic soils (Ashida et al., 2021). The weak positive correlation between Fe_d and maize-derived MAOM ($r_s = 0.42$*) suggests that free Fe (hydr)oxides might partially retain organic matter by surface adsorption (Zhao et al., 2020). However, the insignificant correlation between $Fe_d - Fe_o$ and maize-derived MAOM challenges the direct role of crystalline Fe (hydr)oxides in stabilizing SOM.

The oPOM fraction was a minor destination for maize-derived C (8 ± 4 % of residual maize C). A significant relationship between SOC and $Al_o + Fe_o$ in non-volcanic soils with pH greater than 6 (Ashida et al., 2021) and a significant contribution of Al_o to a linear mixed model predicting SOM stabilization mechanisms (Rasmussen et al., 2018) imply a role for active Al/Fe in stabilizing SOC even in neutral-to-alkaline soils. The predominant contribution of $Al_o + Fe_o$ to maize-derived oPOM ($\beta = 0.62$***; Fig. 5) infers a role for active Al/Fe in organic matter stabilization. Fe (hydr)oxides (Fe_d), such as ferrihydrite, goethite and hematite, and active Al/Fe constituents (Al_o and Fe_o) are especially active in preserving SOM (Lützow et al., 2006; Xue et al., 2020). Rather than direct sorption by (hydr)oxides (Kleber et al., 2007; Kogel-Knabner et al., 2008), an indirect stabilization of organic matter through the promotion of soil aggregate formation is considered an important mechanism (Wagai et al., 2020). However, the non-significant correlation between $Fe_d - Fe_o$ and maize-derived oPOM was found, denying the importance of crystalline Fe (hydr)oxides in preservation of SOM. Active Al/Fe acts as adhesive agents, which can work even in small quantities, binding larger particles (i.e., clay and silt, positively correlated with maize-derived oPOM) to form stable soil aggregates that contribute to preservation of maize transformation products (Figs. 3 and 5). This preservation would be retarded when active Al/Fe is more saturated in topsoil (Table 1), as revealed by the negative contribution of SOC/($Al_o + Fe_o$) to maize-derived oPOM ($\beta = -0.22$*). We assume that the maize-derived oPOM is largely contributed by active Al/Fe, with the contribution of C stabilized as oPOM about 10 % that of MAOM (Fig. 4). This contribution is consistent with a previous study that predicted the relative contribution of active Al to SOM stabilization in neutral-to-slightly alkaline soils (Rasmussen et al., 2018).

The negative correlation of pH with LF and oPOM (Figs. 3 and S12) may suggest retardation of decomposition due to reduced activity of exoenzymes and microbes (Cao et al., 2016; Perez et al., 2002); however, it does not explain the near cessation of maize-derived C mineralization during the later incubation period (Fig. 1). Active Al/Fe, which was elevated in lower pH, wetter soils of lower IGP, and clay and silt fractions, which were also higher in lower IGP due to deposition at downstream, appear to serve as the basic framework for soil aggregate formation (Asano and Wagai, 2014; Churchman et al., 2020; Six et al., 2002), (Table S3, Fig. 5). Hence, soil aggregate formation appears to preferentially preserve the less-degraded maize components as oPOM.

4.3. Identification of maize-derived organic compounds by Py-GC/MS

Most maize-derived organic compounds are considered to be microbially processed and stabilized in the soil based on the molecular compositions determined by Py-GC/MS. Peaks for acetol, 2-hydroxy-3-methyl-2-cyclopenten-1-one, and 3-ethyl-2-hydroxy-2-cyclopenten-1-one (Table S4) are considered pyrolysis products of cellulose (Melligan et al., 2012; Wang et al., 2020; Zhang et al., 2011) and were identified as unique peaks for the maize plant material. These peaks disappeared by the end of the one-year incubation, indicating decomposition of the lignocellulose structure. Even though some metabolites (e.g., neophytadiene in the maize material) have a broad-spectrum antimicrobial ability (Nishanbaev et al., 2019), the plant metabolites and steroids from the maize were effectively decomposed (Tables S4 and S5).

Although lignin is generally considered a recalcitrant substance (Marschner et al., 2008), lignin derived from the maize was absent in subsoil horizons and present in low quantities in topsoil horizons (Table S5). This indicates intensive decomposition of lignin during the incubation. The significant increase of phenols (Table 2, Fig. S15), a decomposition product of lignin and tannin (Leinweber and Schulten, 1999), further confirms decomposition of these recalcitrant materials. Lignin decomposition was enhanced under the C-limited conditions (i.e., low SOC content, Table 1) of subsoil horizons, as exhibited by the disappearance of lignin derived from maize in subsoil horizons relative to its presence in topsoil horizons. This aligns with prior work showing oligotrophic bacteria (e.g., Actinomycetes and Chloroflexi) and lignin-degrading fungi (e.g., Ascomycota) are abundant in subsoil horizons, adapting to utilize recalcitrant organic compounds like lignin in C-limited conditions (Abdel-Hamid et al., 2013; Fierer et al., 2007).

Maize addition improved the quality of soil organic matter as a substrate for microbial utilization as indicated by an increased proportion of FAnE and decreased N-containing compounds (Table 2, Figs. S15 and S17). For example, fatty acids and their esters are highly susceptible to decomposition (Jansen and Wiesenberg, 2017) due to their high

energy density (about 38 kJ g^{-1}) (Sadava et al., 2009). Py-GC/MS identified a large proportion of FAnE (17.9 %) with a major contribution from n-hexadecanoic acid and octadecanoic acid in maize-treated soils (Table 2, Fig. S17). Because of the long incubation period and the virtual cessation of CO_2 release from the added maize near the end of the incubation (Fig. 1), the remaining fatty acids and their esters derived from the added maize are considered to be stabilized by soil mineral interactions, thereby reducing their accessibility/availability as a microbial substrate. The fatty acids and their esters, which microbes would preferentially utilize, appear to be stabilized through association with mineral surfaces and/or occlusion in soil aggregates (Yang et al., 2020).

Nitrogen-containing organic matter originates mainly from microbially-derived organic matter (Buurman and Roscoe, 2011; Carr et al., 2013). Thus, the high relative abundance of N-containing compounds in pyrolysis products of control soil indicates recycling of organic matter by the microbial community (high degree of degradation). In addition to the significant increase of FAnE in maize-treated soils, increases of other labile compounds (e.g., short alkanes) and a decrease of N-containing compounds (Table 2) indicate that the added maize underwent microbial processing and enhanced the quality of SOM. The degraded products were then stabilized by associations with soil minerals (i.e., mainly as MAOM), preventing them from further degradation (Yan et al., 2021). The stronger impact of maize addition on the composition of organic compounds in subsoil versus topsoil horizons is likely due to its lower SOC content and stronger relative stimulation of the microbial community and C cycling by the added carbon substrates.

5. Conclusions

This study revealed that soil properties differentially contributed to SOM mineralization and stabilization processes in neutral-to-alkaline soils. Higher active Al/Fe contents appeared to facilitate aggregation, which inhibited the decomposition of newly introduced maize organic matter. In contrast, higher pH, especially in the upper IGP, promoted C mineralization during the first month of incubation possibly through enhancing microbial accessibility and exoenzyme activities. Higher SOC content and SOC saturation degree, as the main difference between topsoil and subsoil, stimulated mineralization of the added maize by meeting microbial energy demand and limiting stabilization. Residual C from the added maize was mainly stabilized as MAOM (77 $\pm$ 15 %) and oPOM (8 $\pm$ 4 %) underwent microbial processing, as indicated by the disappearance of the unique organic compounds found in maize and increased short alkanes. Higher clay contents directly stabilized more degraded maize as MAOM. Active Al/Fe contributed to the stabilization of maize-derived C, primarily as oPOM, by binding clay and silt as a framework for stable aggregate formation, supporting our first hypothesis. Overall, soils of the drier upper-to-middle IGP have less potential to accumulate organic matter compared with the wetter lower IGP because of their lower clay (and silt) contents, lower active Al/Fe, and higher pH. Maize addition improved SOM quality, as indicated by the increased proportion of fatty acids and decreased N-containing compounds. Thus, the addition of plant materials could be a practical soil management tool for enhancing SOC as the microbially processed OM will be substantially stabilized as MAOM or oPOM, especially in deeper soil horizons having lower C saturation levels with respect to clay + silt and active Al/Fe contents. Meanwhile, the active Al/Fe is low in IGP due to its high pH conditions, which in turn limits the stabilization of OM. Introducing manufactured materials that contain active Al/Fe (e.g., poorly crystalline $Al(OH)_3$) may be beneficial in increasing soil carbon stock, which needs further exploration.

Declaration of Competing Interest

The authors declare that they have no known competing financial interests or personal relationships that could have appeared to influence the work reported in this paper.

Data availability

Data will be made available on request.

Acknowledgments

This work was supported by the JSPS KAKENHI Grant Numbers 17H06171, 19 J14696, 20H04322, 23H03524, and JST SPRING Grant Number JPMJSP2110. We sincerely acknowledge the research partnerships of International Maize and Wheat Improvement Center (CIMMYT) and support of Indian Council of Agricultural Research (ICAR) for this study. We thank Dr. H. S. Jat, Dr. B. Maji, Dr. T. D. Lama (ICAR-Central Soil Salinity Research Institute, Karnal and Canning Town), Dr. Ummed Singh (ICAR-Indian Institute of Pulses Research, Kanpur), Dr. R. K Jat (Borlaug Institute of South Asia, Samastipur, Bihar), Dr. A. K. Sinha (Uttar Banga Krishi Vishwavidyalaya, Cooch Behar, West Bangal), and many other researchers and local people for providing information and kind support for the soil sampling in the study regions.

Appendix A. Supplementary data

Supplementary data to this article can be found online at https://doi.org/10.1016/j.geoderma.2023.116709.

References

Abdel-Hamid, A.M., Solbiati, J.O., Cann, I.K.O., 2013. Chapter One - Insights into lignin degradation and its potential industrial applications. In: S. Sariaslani, G.M. Gadd (Eds.), Advances in Applied Microbiology. Academic Press, pp. 1-28.

Ahn, H.M., et al., 2016. Effects of the timing of a culture temperature reduction on the comprehensive metabolite profiles of Chlorella vulgaris. J. Appl. Phycol. 28, 2641–2650.

Ansari, K.B., Arora, J.S., Chew, J.W., Dauenhauer, P.J., Mushrif, S.H., 2019. Fast pyrolysis of cellulose, hemicellulose, and lignin: Effect of operating temperature on bio-oil yield and composition and insights into the intrinsic pyrolysis chemistry. Ind. Eng. Chem. Res. 58 (35), 15838–15852.

Asano, M., Wagai, R., 2014. Evidence of aggregate hierarchy at micro- to submicron scales in an allophanic Andisol. Geoderma 216, 62–74.

Ashida, K., et al., 2021. Quantitative relationship between organic carbon and geochemical properties in tropical surface and subsurface soils. Biogeochemistry 155, 77–95.

Beare, M.H., Hendrix, P.F., Cabrera, M.L., Coleman, D.C., 1994. Aggregate-Protected and Unprotected Organic Matter Pools in Conventional- and No-Tillage Soils. Soil Sci. Soc. Am. J. 58 (3), 787–795.

Beare, M.H., McNeill, S.J., Curtin, D., Parfitt, R.L., Jones, H.S., Dodd, M.B., Sharp, J., 2014. Estimating the organic carbon stabilisation capacity and saturation deficit of soils: a New Zealand case study. Biogeochemistry 120 (1–3), 71–87.

Blagodatskaya, E., Kuzyakov, Y., 2008. Mechanisms of real and apparent priming effects and their dependence on soil microbial biomass and community structure: Critical review. Biol. Fertil. Soils 45 (2), 115–131.

Blakemore, L.C., 1987. Extractable iron, aluminium and silicon. In Methods for Chemical Analysis of Soils. NZ Soil Bureau Scientific Report 80, 71–76.

Buurman, P., Peterse, F., Almendros Martin, G., 2007. Soil organic matter chemistry in allophanic soils: a pyrolysis-GC/MS study of a Costa Rican Andosol catena. Eur. J. Soil Sci. 58 (6), 1330–1347.

Buurman, P., Roscoe, R., 2011. Different chemical composition of free light, occluded light and extractable SOM fractions in soils of Cerrado and tilled and untilled fields, Minas Gerais, Brazil: a pyrolysis-GC/MS study. Eur. J. Soil Sci. 62 (2), 253–266.

Cao, H., et al., 2016. Soil pH, total phosphorus, climate and distance are the major factors influencing microbial activity at a regional spatial scale. Sci. Rep. 6, 25815.

Carr, A.S., et al., 2013. Biome-scale characterisation and differentiation of semi-arid and arid zone soil organic matter compositions using pyrolysis–GC/MS analysis. Geoderma 200–201, 189–201.

Chen, H., et al., 2018. Integration of an automated identification-quantification pipeline and statistical techniques for pyrolysis GC/MS tracking of the molecular fingerprints of natural organic matter. J. Anal. Appl. Pyrol. 134, 371–380.

Chen, L., et al., 2019. Regulation of priming effect by soil organic matter stability over a broad geographic scale. Nat. Commun. 10, 1–10.

Churchman, G.J., Singh, M., Schapel, A., Sarkar, B., Bolan, N., 2020. Clay minerals as the key to the sequestration of carbon in soils. Clay Clay Miner. 68 (2), 135–143.

Coleman, D.C., Callaham, M.A., Crossley, D.A., 2018. Chapter 3 - Secondary Production: Activities of Heterotrophic Organisms—Microbes. In: D.C. Coleman, M.A. Callaham, D.A. Crossley (Eds.), Fundamentals of Soil Ecology (Third Edition). Academic Press, pp. 47-76.

Curtin, D., Peterson, M.E., Anderson, C.R., 2016. pH-dependence of organic matter solubility: Base type effects on dissolved organic C, N, P, and S in soils with contrasting mineralogy. Geoderma 271, 161–172.

Dai, S.S., et al., 2022. Faster carbon turnover in topsoil with straw addition is less beneficial to carbon sequestration than subsoil and mixed soil. Soil Sci. Soc. Am. J. 86, 1431–1443.
Derenne, S., Quénéa, K., 2015. Analytical pyrolysis as a tool to probe soil organic matter. J. Anal. Appl. Pyrol. 111, 108–120.
Dungait, J.A.J., et al., 2011. Variable responses of the soil microbial biomass to trace concentrations of 13C-labelled glucose, using 13C-PLFA analysis. Eur. J. Soil Sci. 62, 117–126.
Dungait, J.A., Hopkins, D.W., Gregory, A.S., Whitmore, A.P., 2012. Soil organic matter turnover is governed by accessibility not recalcitrance. Glob. Chang. Biol. 18 (6), 1781–1796.
Feller, C., Beare, M.H., 1997. Physical control of soil organic matter dynamics in the tropics. Geoderma 79 (1), 69–116.
Feng, W., Plante, A.F., Six, J., 2011. Improving estimates of maximal organic carbon stabilization by fine soil particles. Biogeochemistry 112 (1–3), 81–93.
Fick, S.E., Hijmans, R.J., 2017. WorldClim 2: new 1-km spatial resolution climate surfaces for global land areas. Int. J. Climatol. 37 (12), 4302–4315.
Fierer, N., Bradford, M.A., Jackson, R.B., 2007. Toward an ecological classification of soil bacteria. Ecology 88 (6), 1354–1364.
Fujii, K., et al., 2020. A comparison of lignin-degrading enzyme activities in forest floor layers across a global climatic gradient. Soil Ecology Letters 2, 281–294.
Garrido, E., Matus, F., 2012. Are organo-mineral complexes and allophane content determinant factors for the carbon level in Chilean volcanic soils? Catena 92, 106–112.
Gee, G.W., Or, D., 2002. 2.4 Particle-size analysis. In: J.H. Dane, G.C. Topp (Eds.), Methods of Soil Analysis. SSSA Book Series. Soil Science Society of America, pp. 255-293.
Girona-García, A., Badía-Villas, D., Jiménez-Morillo, N.T., González-Pérez, J.A., 2019. Changes in soil organic matter composition after Scots pine afforestation in a native European beech forest revealed by analytical pyrolysis (Py-GC/MS). Sci. Total Environ. 691, 1155–1161.
Hair, J.F. et al., 2021. The SEMinR Package. in: Hair Jr, J.F. et al. (Eds.), Partial Least Squares Structural Equation Modeling (PLS-SEM) Using R: A Workbook. Springer International Publishing, Cham, pp. 49-74.
IUSS Working Group WRB, 2022. World Reference Base for Soil Resources, International soil classification system for naming soils and creating legends for soil maps. International Union of Soil Sciences (IUSS), Vienna, Austria.
Jansen, B., Wiesenberg, G.L.B., 2017. Opportunities and limitations related to the application of plant-derived lipid molecular proxies in soil science. SOIL 3 (4), 211–234.
Jobbagy, E.G., Jackson, R.B., 2000. The vertical distribution of soil organic carbon and its relation to climate and vegetation. Ecol. Appl. 10 (2), 423–436.
Kadono, A., Funakawa, S., Kosaki, T., 2008. Factors controlling mineralization of soil organic matter in the Eurasian steppe. Soil Biol. Biochem. 40 (4), 947–955.
Kleber, M., Sollins, P., Sutton, R., 2007. A conceptual model of organo-mineral interactions in soils: self-assembly of organic molecular fragments into zonal structures on mineral surfaces. Biogeochemistry 85 (1), 9–24.
Koch, A.L., 2001. Oligotrophs versus copiotrophs. Bioessays 23 (7), 657–661.
Kogel-Knabner, I., et al., 2008. Organo-mineral associations in temperate soils: Integrating biology, mineralogy, and organic matter chemistry. J. Plant Nutr. Soil Sci. 171 (1), 61–82.
Kuzyakov, Y., 2010. Priming effects: Interactions between living and dead organic matter. Soil Biol. Biochem. 42 (9), 1363–1371.
Lal, R., 2004. Soil carbon sequestration in India. Clim. Change 65 (3), 277–296.
Lal, R., 2010. Managing soils and ecosystems for mitigating anthropogenic carbon emissions and advancing global food security. Bioscience 60 (9), 708–721.
Lal, R., 2018. Digging deeper: A holistic perspective of factors affecting soil organic carbon sequestration in agroecosystems. Glob. Chang. Biol. 24 (8), 3285–3301.
Leinweber, P., Schulten, H.R., 1999. Advances in analytical pyrolysis of soil organic matter. J. Anal. Appl. Pyrol. 49 (1), 359–383.
Lu, X., et al., 2021. Nitrogen deposition accelerates soil carbon sequestration in tropical forests. Proceedings of the National Academy of Sciences 118 (16), e2020790118.
Lützow, M.V., et al., 2006. Stabilization of organic matter in temperate soils: mechanisms and their relevance under different soil conditions - a review. Eur. J. Soil Sci. 57 (4), 426–445.
Lyu, H., et al., 2021b. Factors controlling sizes and stabilities of subsoil organic carbon pools in tropical volcanic soils. Sci. Total Environ. 769, 144842.
Lyu, H., et al., 2022. Climatic controls on soil clay mineral distributions in humid volcanic regions of Sumatra and Java. Indonesia. Geoderma 425, 116058.
Lyu, H., Watanabe, T., Kilasara, M., Hartono, A., Funakawa, S., 2021a. Soil organic carbon pools controlled by climate and geochemistry in tropical volcanic regions. Sci. Total Environ. 761, 143277.
Ma, Q., Watanabe, T., Zheng, J., Funakawa, S., 2021. Interactive effects of crop residue quality and nitrogen fertilization on soil organic carbon priming in agricultural soils. J. Soil. Sediment. 21 (1), 83–95.
Manzoni, S., Taylor, P., Richter, A., Porporato, A., Ågren, G.I., 2012. Environmental and stoichiometric controls on microbial carbon-use efficiency in soils. New Phytol. 196 (1), 79–91.
Marschner, B., et al., 2008. How relevant is recalcitrance for the stabilization of organic matter in soils? J. Plant Nutr. Soil Sci. 171 (1), 91–110.
McNally, S.R., et al., 2017. Soil carbon sequestration potential of permanent pasture and continuous cropping soils in New Zealand. Glob Chang. Biol. 23 (11), 4544–4555.
McNally, S.R., et al., 2018. Assessing the vulnerability of organic matter to C mineralisation in pasture and cropping soils of New Zealand. Soil Res. 56 (5), 481–490.
Melligan, F., Hayes, M.H.B., Kwapinski, W., Leahy, J.J., 2012. Hydro-pyrolysis of biomass and online catalytic vapor upgrading with Ni-ZSM-5 and Ni-MCM-41. Energy Fuel 26 (10), 6080–6090.
Nakagawa-Izumi, A., et al., 2017. Characterization of syringyl and guaiacyl lignins in thermomechanical pulp from oil palm empty fruit bunch by pyrolysis-gas chromatography-mass spectrometry using ion intensity calibration. Ind. Crop. Prod. 95, 615–620.
Neina, D., 2019. The role of soil pH in plant nutrition and soil remediation. Appl. Environ. Soil Sci. 2019, 9.
Nishanbaev, S., et al., 2019. Component composition of the extracts and essential oils from the Alhagi canescens, growing in Uzbekistan and their antimicrobial activity. Nat. Prod. Res. 33 (23), 3417–3420.
Oades, J., Waters, A., 1991. Aggregate Hierarchy in Soils. Soil Research 29 (6), 815–828.
Pal, D.K., Bhattacharyya, T., Srivastava, P., Chandran, P., Ray, S.K., 2009. Soils of the Indo-Gangetic Plains: their historical perspective and management. Curr. Sci. 96 (9), 1193–1202.
Paul, E., Morris, S., Bohm, S., 2001. The determination of soil C pool sizes and turnover rates: Biophysical fractionation and tracers, Assessment Methods for Soil Carbon, CRC Press, Boca Raton, pp. 193-206.
Perez, J., Munoz-Dorado, J., de la Rubia, T., Martinez, J., 2002. Biodegradation and biological treatments of cellulose, hemicellulose and lignin: an overview. Int. Microbiol. 5 (2), 53–63.
Picó, Y., Barceló, D., 2020. Pyrolysis gas chromatography-mass spectrometry in environmental analysis: Focus on organic matter and microplastics. TrAC Trends Anal. Chem. 130, 115964.
Possinger, A.R., et al., 2021. Climate effects on subsoil carbon loss mediated by soil chemistry. Environ. Sci. Tech. 55 (23), 16224–16235.
Puissant, J., et al., 2019. The pH optimum of soil exoenzymes adapt to long term changes in soil pH. Soil Biol. Biochem. 138, 107601.
Rakhsh, F., Golchin, A., Al Agha, A.B., Alamdari, P.J.G., 2017. Effects of exchangeable cations, mineralogy and clay content on the mineralization of plant residue carbon. Geoderma 307, 150–158.
Rasmussen, C., Heckman, K., Wieder, W.R., Keiluweit, M., Lawrence, C.R., Berhe, A.A., Blankinship, J.C., Crow, S.E., Druhan, J.L., Pries, C.E.H., Marin-Spiotta, E., Plante, A. F., Schadel, C., Schimel, J.P., Sierra, C.A., Thompson, A., Wagai, R., 2018. Beyond clay: towards an improved set of variables for predicting soil organic matter content. Biogeochemistry 137 (3), 297–306.
Rennert, T., 2019. Wet-chemical extractions to characterise pedogenic Al and Fe species – a critical review. Soil Res. 57 (1), 1–16.
Rodrigues, L.A.T., et al., 2022a. Carbon sequestration capacity in no-till soil decreases in the long-term due to saturation of fine silt plus clay-size fraction. Geoderma 412, 115711.
Rodrigues, L.A.T., et al., 2022b. Carbon saturation deficit and litter quality drive the stabilization of litter-derived C in mineral-associated organic matter in long-term no-till soil. Catena 219, 106590.
Rousk, J., Brookes, P.C., Bååth, E., 2009. Contrasting soil pH effects on fungal and bacterial growth suggest functional redundancy in carbon mineralization. Appl. Environ. Microbiol. 75 (6), 1589–1596.
Rowley, M.C., Grand, S., Verrecchia, E.P., 2018. Calcium-mediated stabilisation of soil organic carbon. Biogeochemistry 137 (1–2), 27–49.
Sadava, D.E., Hillis, D.M., Heller, H.C., 2009. Life: The Science of Biology, 2. Macmillan, London.
Saifuddin, M., Bhatnagar, J.M., Segrè, D., Finzi, A.C., 2019. Microbial carbon use efficiency predicted from genome-scale metabolic models. Nat. Commun. 10 (1), 3568.
Shahbaz, M., et al., 2017. Microbial decomposition of soil organic matter is mediated by quality and quantity of crop residues: mechanisms and thresholds. Biol. Fertil. Soils 53 (3), 287–301.
Six, J., et al., 2002. Soil organic matter, biota and aggregation in temperate and tropical soils - Effects of no-tillage. Agronomie 22 (7–8), 755–775.
Soil Survey Laboratory Staff, 1996. Soil survey laboratory methods manual. US Gov. Print. Office, Washington, DC.
Stewart, C.E., Paustian, K., Conant, R.T., Plante, A.F., Six, J., 2008. Soil carbon saturation: Evaluation and corroboration by long-term incubations. Soil Biol. Biochem. 40 (7), 1741–1750.
Sukhoveeva, O.E., 2022. Input of organic carbon to soil with post-harvest crop residues. Eurasian Soil Sci. 55 (6), 810–818.
Tiessen, H., Cuevas, E., Chacon, P., 1994. The role of soil organic matter in sustaining soil fertility. Nature 371 (6500), 783–785.
Tisdall, J., 2020. Formation of soil aggregates and accumulation of soil organic matter, Structure and organic matter storage in agricultural soils. CRC Press 57–96.
Tokarski, D., et al., 2020. Linking thermogravimetric data with soil organic carbon fractions. Geoderma 362, 114124.
Trinsoutrot, I., et al., 2000. Biochemical quality of crop residues and carbon and nitrogen mineralization kinetics under nonlimiting nitrogen conditions. Soil Sci. Soc. Am. J. 64 (3), 918–926.
Ugolini, F.C., Dahlgren, R.A., 2002. Soil development in volcanic ash. Global Environ. Res.-Englilsh Ed. 6 (2), 69–82.
Vågen, T.G., Lal, R., Singh, B.R., 2005. Soil carbon sequestration in sub-Saharan Africa: A review. Land Degrad. Dev. 16 (1), 53–71.
Wagai, R., Kajiura, M., Asano, M., 2020. Iron and aluminum association with microbially processed organic matter via meso-density aggregate formation across soils: organo-metallic glue hypothesis. Soil 2020, 1–42.
Wang, Q., et al., 2020. Initial pyrolysis mechanism and product formation of cellulose: An experimental and density functional theory(DFT) study. Sci. Rep. 10 (1), 3626.

Wang, S., Guo, X., Liang, T., Zhou, Y., Luo, Z., 2012. Mechanism research on cellulose pyrolysis by Py-GC/MS and subsequent density functional theory studies. Bioresour. Technol. 104, 722–728.
West, T.O., Marland, G., 2003. Net carbon flux from agriculture: Carbon emissions, carbon sequestration, crop yield, and land-use change. Biogeochemistry 63 (1), 73–83.
Wu, L., et al., 2020. Soil carbon balance by priming differs with single versus repeated addition of glucose and soil fertility level. Soil Biol. Biochem. 148, 107913.
Xue, B., et al., 2020. Straw management influences the stabilization of organic carbon by Fe (oxyhydr)oxides in soil aggregates. Geoderma 358.
Yan, M., Zhang, X., Liu, K., Lou, Y., Wang, Y., 2021. Particle size primarily shifts chemical composition of organic matter under long-term fertilization in paddy soil. Eur. J. Soil Sci. 73 (1).
Yang, S., Jansen, B., Absalah, S., Kalbitz, K., Cammeraat, E.L.H., 2020. Selective stabilization of soil fatty acids related to their carbon chain length and presence of double bonds in the Peruvian Andes. Geoderma 373, 114414.
Yu, G., et al., 2017. Mineral availability as a key regulator of soil carbon storage. Environ. Sci. Tech. 51 (9), 4960–4969.
Zhang, Y.L., et al., 2018. Structural evidence for soil organic matter turnover following glucose addition and microbial controls over soil carbon change at different horizons of a Mollisol. Soil Biol. Biochem. 119, 63–73.
Zhang, H., Cheng, Y.T., Vispute, T.P., Xiao, R., Huber, G.W., 2011. Catalytic conversion of biomass-derived feedstocks into olefins and aromatics with ZSM-5: the hydrogen to carbon effective ratio. Energ. Environ. Sci. 4 (6), 2297–2307.
Zhao, Q., et al., 2020. Strong mineralogic control of soil organic matter composition in response to nutrient addition across diverse grassland sites. Sci. Total Environ. 736, 137839.
Zhao, J., Li, R., Li, X., Tian, L., 2017. Environmental controls on soil respiration in alpine meadow along a large altitudinal gradient on the central Tibetan Plateau. Catena 159, 84–92.
Zhou, W., Han, G., Liu, M., Li, X., 2019. Effects of soil pH and texture on soil carbon and nitrogen in soil profiles under different land uses in Mun River Basin, Northeast Thailand. Peerj 7, e7880.